

NASA TECHNICAL
MEMORANDUM

NASA TM X-53468

May 26, 1966

NASA TM X-53468

AN ORBITING DENSITY MEASURING INSTRUMENT

By D. A. Wallace, K. W. Rogers, J. B. Wainwright
and R. L. Chuan

FACILITY FORM 602	N66 33539	
	(ACCESSION NUMBER)	(THRU)
	57	1
	(PAGES)	(CODE)
	TMX-53468	14
	(NASA CR OR TMX OR AD NUMBER)	(CATEGORY)

NASA

*George C. Marshall
Space Flight Center,
Huntsville, Alabama*

GPO PRICE \$ _____

CFSTI PRICE(S) \$ _____

Hard copy (HC) 2.50

Microfiche (MF) 1.50

TECHNICAL MEMORANDUM X-53468

AN ORBITING DENSITY MEASURING INSTRUMENT

By

D. A. Wallace, K. W. Rogers,

J. B. Wainwright and R. L. Chuan

George C. Marshall Space Flight Center

Huntsville, Alabama

ABSTRACT

33539

A design study has been conducted for a direct air density measuring device that can be carried onboard an orbiting spacecraft in the altitude range from 140 to 280 km. The resulting design calls for a free molecular cryopumped gas collector of nearly unity capture coefficient, using an orifice collector and a cooled piezoelectric crystal acting as a micro-balance. Refrigeration is by heat sinks pre-conditioned before launch. Measurement is through beat-frequency (between cryopumping crystal and a variable oscillator) converted to DC voltage, thence to telemetry.

NASA - GEORGE C. MARSHALL SPACE FLIGHT CENTER

Technical Memorandum X-53468

May 26, 1966

AN ORBITING DENSITY MEASURING INSTRUMENT

By

D. A. Wallace, K. W. Rogers,

J. B. Wainwright and R. L. Chuan*

*This study was completed under NASA Contract NAS8-20213 with the Celestial Research Corporation, 511 Mission Street, South Pasadena, California.

SPACE ENVIRONMENT BRANCH
AEROSPACE ENVIRONMENT DIVISION
AERO-ASTRODYNAMICS LABORATORY
RESEARCH AND DEVELOPMENT OPERATIONS

TABLE OF CONTENTS

	<u>Page</u>
I. INTRODUCTION.....	1
II. BASIC SCHEME OF DIRECT DENSITOMETRY BY CRYOPUMPING.....	2
III. COLLECTION PROCESS.....	4
A. Molecular Flux Measurement and Capture Efficiency...	4
B. Surface Sticking Coefficient.....	6
C. Capture Coefficient.....	6
D. Cylindrical Collector.....	7
E. Orifice Collector.....	8
F. Noncondensable Gases.....	9
IV. MEASUREMENT TECHNIQUE AND ACCURACY.....	10
A. Intermittent Collection.....	10
1. Minimum Collection Time.....	10
2. Altitude Range.....	11
3. Measurement Accuracy.....	12
B. Continuous Collection.....	14
1. Maximum Collection Time.....	14
2. Altitude Range.....	16
3. Measurement Accuracy.....	18
V. COOLANT SYSTEM.....	19
A. Intermittent Collection.....	19
1. Cooling Scheme.....	19
2. Refrigeration Requirements.....	20
(a) Cooldown Requirement.....	20
(b) Condensed Gas Requirement.....	21
(c) Helium Reservoir.....	22
B. Continuous Collection.....	22
1. Coolant Scheme.....	22
2. Refrigeration Requirements.....	23
(a) Crystal Sensor.....	23
(b) Collector Wall.....	25
VI. SUMMARY DESCRIPTION OF RECOMMENDED SYSTEM.....	27
APPENDIX A. CAPTURE COEFFICIENT.....	35
APPENDIX B. ACCOMMODATION COEFFICIENT.....	39
APPENDIX C. SPUTTERING.....	41
APPENDIX D. REFRIGERATION BY HYDROGEN SUBLIMATION.....	43

LIST OF ILLUSTRATIONS

<u>Figure</u>	<u>Title</u>	<u>Page</u>
1	Cryopanel Normal to the Airstream.....	29
2	Cylindrical Cryopanel Aligned with Airstream...	29
3	Effect of L/D and Speed Ratio.....	30
4	Cylindrical Cryopanel with Reduced Inlet Area..	30
5	General Collector Configuration.....	31
6	Measurement Pressure vs Collection Time Fraction.....	31
7	Crystal Sensor Frequency Shift Measurement System.....	32
8	Intermittent Collector.....	33
9	Continuous Collector.....	33
A-1	Variations of Sticking Coefficient with Temperature.....	37
A-2	One-Dimensional Model of Surface Interaction...	37
B-1	Accommodation Coefficient Variation.....	40
C-1	Yield vs Energy Ratio.....	42
D-1	Solid Phase Vapor Pressure.....	43
D-2	Hydrogen Sublimation Coolant System.....	46

TECHNICAL MEMORANDUM X-53468

AN ORBITING DENSITY MEASURING INSTRUMENT

SUMMARY

A design study has been conducted for a direct air density measuring device that can be carried onboard an orbiting spacecraft in the altitude range from 140 to 280 km. The resulting design calls for a free molecular cryopumped gas collector of nearly unity capture coefficient, using an orifice collector and a cooled piezoelectric crystal acting as a micro-balance. Refrigeration is by heat sinks pre-conditioned before launch. Measurement is through beat-frequency (between cryopumping crystal and a variable oscillator) converted to DC voltage, thence to telemetry.

I. INTRODUCTION

The need for the accurate prediction of spacecraft orbit decay has generated a need for an accurate determination of the pertinent atmospheric property - mass density, i.e., mass per unit volume, at the orbital altitudes of concern. The most direct way of measuring this quantity is to proceed by its definition, namely, to measure the mass of gas, regardless of composition, contained in a known ambient volume at orbital altitudes. Any technique attempting to make such a determination must be capable of (1) collecting the mass of gas, (2) sensing the collected mass, (3) determining the volume from which the mass was collected, and (4) determining spatial position.

Tracking provides the spatial position data, as well as spacecraft velocity; thus, an onboard instrument must consist of components capable of collection, sensing, and volume determination.

Celestial Research Corporation has conducted a feasibility and design study to develop an air density measuring instrument based primarily on existing technology, so that the successful conclusion of the study would lead expeditiously to appropriate flight hardware without extensive research and development efforts. This report documents the results of the study on two possible methods and recommends one for hardware development.

The nominal altitude considered is 180 kilometers; the vehicle assumed is one similar to the Saturn S-IVB.

II. BASIC SCHEME OF DIRECT DENSITOMETRY BY CRYOPUMPING

The design approach is based upon the fact that a gas collection element aligned parallel to the spacecraft flight direction will sweep out an ambient gas volume

$$V_a = A_o u t, \quad (1)$$

where A_o is the projected inlet area of the collector, u is the spacecraft velocity, and t is the time of collection.

The collection time is primarily a function of the mass sensing technique which in turn is determined by available instrumentation. Two approaches were investigated which more or less bracketed the possibilities, in that one instrument, a pressure transducer, relied on an intermittent collection cycle with pressure amplification, while the other instrument, a cryogenically cooled quartz crystal micro-balance, could continuously collect and sense the incoming mass flux. Each of these measurement techniques had its advantages and shortcomings which will be discussed in detail in a later section.

The scheme for the intermittent measurement technique involves the collection of ambient gas for some specified time, the valving off of the collector with the captured cryogenically pumped gas, and the vaporization of the collected solid condensate by warming the collector to a known temperature. We can then determine the ambient mass density, ρ_a , knowing the collector gas pressure as measured by the pressure transducer, the collector gas temperature, T_m , which is the same as the collector wall, the gas constant, R_m , the collector measurement volume, V_m , and the ambient collected volume, V_a , from equation (1).

$$\rho_a = \rho_m \frac{V_m}{V_a} = \frac{V_m}{V_a} \frac{P_m}{R_m T_m}$$

or

$$\rho_a = \frac{V_c + V_g}{A_o u t} \frac{P_m}{R_m T_m} \quad (2)$$

where

m = combined measurement volume

c = collector

g = pressure gage

a = ambient.

Pressure can be amplified to readily measurable levels by adjustment of the inlet area, the collection time, and the measurement volume. The measurement cycle is completed by opening the collector inlet valve, thus venting the collected gas out to the free stream atmosphere and reducing the residual collector pressure to a negligible level relative to the pressure level during measurement.

The continuous mass measurement technique is more direct in that a cryogenically cooled quartz crystal cryopumps the entering mass onto the resonating crystal which responds to changes in system mass by a shift in the resonant frequency; thus, mass flux is measured directly without intermediate measurements or calculations. The frequency shift is approximately a linear function of the collected mass until the shift becomes approximately 1 percent of the crystal's resonant frequency. For a crystal in thickness shear resonance, the sensitivity, i.e., the frequency shift with mass change, can be expressed as a function of the resonant frequency over the applicable linear range:

$$\Delta f = C \Delta m f_r^2, \quad (3)$$

where

C = constant

f_r = basic resonant frequency

Δm = collected mass

Δf = frequency shift.

The question of whether or not the crystal need be thermally cycled to clean the crystal of accumulated condensate and thus avoid loading the crystal beyond its linear response range is influenced not only by orbital parameters but also by the required collector geometry for high capture coefficients and by the frequency shift sensing equipment. This will be discussed in detail in a later section.

The refrigeration source and coolant system for the cryopumping of the collected mass is dependent upon the measurement technique. In the case of intermittent collection and pressure amplification, the entire collector wall is held at a low temperature during the collection cycle such that condensation of the entering gas molecules occurs with resultant condensate vapor pressure at least an order of magnitude below the ambient pressure.

For air constituents, this means temperatures on the order of 20°K which can be obtained with either liquid hydrogen or helium as the refrigeration source. Once the gas sample has been collected, the collector wall, which has previously been functioning as a cryopump, must be raised to a temperature level which will again vaporize the gas sample for the pressure measurement. Once the pressure measurement is made, the gas sample is vented, and the collector is again cooled to approximately 20°K and the inlet valve reopened for the next gas sample. This thermal cycling calls for a rather sophisticated refrigeration system which will be discussed later.

In the case of continuous collection, the quartz crystal, which becomes the cryopumping surface, must be cooled to temperatures below 20°K to collect the incoming mass. The collector walls are held at an intermediate temperature - high enough to avoid cryopumping yet low enough to reduce the energy level of impinging molecules to achieve eventual condensation on the crystal. This results in a relatively simple coolant system, since the heat load to both the collector walls and the crystal remains constant throughout the flight. The use of the crystal in this manner, i.e., as a continuous mass collector, is contingent upon the ability of the sensing instrumentation to measure percentage-wise very small frequency shifts, thus avoiding a thermal cycling of the crystal.

The individual densitometer components will be studied separately in the following sections, and an overall system error analysis will be presented for the recommended system design.

III. COLLECTION PROCESS

A. Molecular Flux Measurement and Capture Efficiency

The first step in this type of density meter is the collection phase. In this phase the free stream molecules are captured by condensation on a cryopump. As a simple example, consider a cryopump consisting of a flat panel that is extended normal to the free stream (see Figure 1). If the flow is free molecular with respect to the cryopump, and if the molecules that impinge on the front face of the cryopanel are condensed, the mass will accumulate at a rate given by

$$N_c = N_\infty = n_\infty \sqrt{2kT_\infty/M} \frac{\chi(S)}{2\sqrt{\pi}} \quad (4)$$

where

N = molecular flux (molecules/sec-cm²)

n = density (molecules/cm³)

k = Boltzmann constant

T = temperature

M = molecular weight

S = speed ratio = $\frac{u}{\sqrt{2 \frac{k}{M} T}}$

$$\chi(S) = \exp(-S^2) + \sqrt{\pi} S(1 + \operatorname{erf} S).$$

Thus, by measuring the mass that has been collected over a known period of time (t), an average free stream molecular flux can be determined. If s , T and M are constant over that time period, the average free stream density can be determined from equation (4).

If all of the impinging molecules are not condensed, equation (4) must be modified. Assuming that only a fraction (ϕ) of the impinging molecules are captured, equation (4) becomes

$$N_c = \phi N, \quad (5)$$

where

ϕ = captured coefficient.

Thus, in order to relate the measured collection rate and the free stream density, the capture coefficient must be known. If there is no interaction between the incoming molecules and the molecules that rebounded from the plate without being captured, the capture coefficient (ϕ) is equal to the surface sticking coefficient (σ). The sticking coefficient is a more fundamental parameter since it is the probability that an incident molecule will be captured during a collision with a cryopump. In this application, the interaction between rebounding and incident

molecules is negligible (since the mean free paths involved are always much larger than the collector dimensions) so that in the case of the flat plate, $\phi = \sigma$.

B. Surface Sticking Coefficient

It is apparent from equations (4) and (5) that, for the simple flat plate configuration, the uncertainty in the measurement of the free stream density will be no less than the uncertainty in the sticking coefficient. The sticking coefficient is closely related to the critical energy level (E_c). This is the average maximum energy level that an incident molecule can have and still be captured during a collision with the wall. It is shown in Appendix A that there is considerable uncertainty in the value of the critical energy level, but it appears to be in the range of 1 to 25 times the binding energy of the molecule. The binding energy (E_b) is essentially the energy that must be expended to remove a condensed molecule from the condensate layer. This is comparable to the heat of vaporization or about .07 eV for a nitrogen molecule. In contrast, the energy associated with incident molecules (E_i) during orbital conditions is about 9 eV. Since the incident energy is 4 or 5 times the estimated upper limit of the critical energy level, it is doubtful that any significant number of the incident molecules will stick on this simple flat-plate cryopump.

The negligible value for the sticking coefficient of incident molecules with orbital energy levels represents a fundamental limitation on the flat-plate cryopump when operated in free molecular flow conditions.

C. Capture Coefficient

While the sticking coefficient is independent of the cryopump configuration, the capture coefficient is not, and can be increased. For example, consider a cryopump that consists of the interior of a cylinder and an end disc as shown in Figure 2. By aligning the cylinder with the free stream, the directed velocity of the molecules will cause most of the molecules to have their first collision deep inside the tube. While these molecules will probably not stick on this first collision, they will have a high probability of having several more collisions with the walls before passing back out the entrance. During each collision, the energy level will decrease, so that, if there are enough collisions, the energy level will fall below the critical level and the molecule will be captured. This is the same technique discussed by Wallace and Rogers [1] as a method for maintaining a low background pressure while test firing a rocket motor.

The feasibility of this technique depends upon the energy lost per collision, or the accommodation coefficient (α), which is the ratio of the energy lost in a collision to the maximum energy that could be lost.

$$\alpha = \frac{E_i - E_{\text{off}}}{E_i - E_{\text{wall}}} \quad (6)$$

Since there is a lack of experimental data for the accommodation coefficient of a high energy gas impinging on a condensate layer, it is necessary to extrapolate the available data using theoretical results as a guide. As outlined in Appendix B, this approach yields an estimate of $\alpha = .77$. This is assumed to be independent of the molecular energy level, so that the number of collisions (ν) required to lower the energy level to the critical value can be obtained from

$$(1 - \alpha)^\nu = \frac{E_c}{E_i} \quad (7)$$

When this is evaluated with $\alpha = .77$, $E_c = .07$ and $E_i = 9$, it is found that $\nu = 3.3$. Thus, 3 or 4 collisions would be required to lower the energy level to the point that the molecule would stick on the next collision with the cold wall.

D. Cylindrical Collector

An analysis based on a Monte Carlo program developed by Ballance [2] has been made of a series of cylindrical cryopumps operating at $S = \infty$ and $S = 10$. In using this approach, it is assumed that all molecular rebounds are diffuse. Typical results are shown in Figure 3. It is seen that, when $S = \infty$, there is a continuing benefit from increasing the L/D of the cylinder. This is to be expected, since for $S = \infty$, all the incident molecules strike the aft disc; therefore, increasing the tube length increases the distances the molecules must travel to the opening. Increasing this distance increases the probability that a molecule will have enough collisions to decrease the energy below the critical energy level so that it will be captured.

Increasing the L/D of the cylinder is also effective when $S = 10$ if L/D is small. However, if the L/D is large, there is no significant benefit from further increases. In the case of a large L/D , the capture coefficient is limited by the loss of those molecules that initially strike

the cylindrical walls near the inlet. Since this loss is essentially independent of the L/D of the cylinder, there is no benefit in increasing the ratio beyond $L/D = 6$. From Figure 3 it appears that there is an uncertainty of at least 5 - 10 percent in the value of the capture coefficient for a cylindrical cryopump.

Consideration of the losses due to sputtering of the condensate layer by the high energy incident molecules also increases this uncertainty. No experimental data are available for the sputtering of an air condensate layer by incident air molecules, but a crude correlation (see Appendix C) based on results of metallic sputtering indicates that the yield would be of the order of unity; i.e., each high energy incoming molecule would sputter one condensate molecule. While it appears that neither of these molecules would have sufficient energy to cause further sputtering, this initial sputtering increases the uncertainty of the capture coefficient by about 5 percent.

Since the estimated uncertainty is quite high and becomes even higher if angle of attack effects are considered, this cylindrical configuration does not appear satisfactory for use in an orbital collector, unless the uncertainties can be further reduced by some extensive experimental investigation. Since there are no facilities that can properly duplicate orbital conditions, it is advisable to find a configuration that is less sensitive to the uncertainties in sticking coefficient, accommodation coefficient, and sputtering yield.

E. Orifice Collector

The capture coefficient based on the inlet area can be further increased by using an inlet diameter that is smaller than the tube diameter (Figure 4). For example, if the inlet diameter is $1/3$ of the tube diameter, the molecular loss rate is reduced to about 15 percent of that obtained when the inlet diameter is equal to the tube diameter. This approach has the further advantage that the collector is much less sensitive to angle-of-attack effects. On the other hand, the reduced inlet area results in a lower flow rate into the collector, so that for a fixed altitude either the collection time or the gage sensitivity must be increased. These factors will be considered in more detail in another section.

While this reduced inlet area configuration does decrease the uncertainties in the capture coefficient, the configuration shown in Figure 5 reduces the uncertainties even further. In this configuration, the molecules that enter through A_0 impinge on the wall A_5 that is cold but not cold enough to cryopump. After a sufficient number of collisions with this cold wall ($T < 80^\circ\text{K}$), the energy level of the molecules is below the critical value and the molecules will condense upon their next collision with A_C , the cryopumping surface ($T < 20^\circ\text{K}$). During the

collisions that are required to cool the molecules below the critical energy level, some molecules will pass out through the inlet. If the rebounds are diffuse, the fraction of the molecules lost per wall collision is A_0/A_S . If there are ν collisions required to cool the molecules, the total losses during this phase will be $\nu A_0/A_S$.

There will also be molecular losses during the condensation phase. These fractional losses will be approximately equal to A_0/A_C . Thus the total inlet losses during collection will be $\nu A_0/A_S + A_0/A_C$. To minimize errors, it is necessary that these losses should not exceed 1 to 2 percent. This requires that A_0/A_C and $\nu A_0/A_S$ each be about 0.01.

The value of ν depends upon the thermal accommodation coefficient. This in turn varies with the intermolecular force between the gas and the wall, and the ratio of the molecular weights. If the system is fabricated from aluminum, the wall molecular weight is comparable to that of the collected gas. Furthermore, the intermolecular force between the gas and the metal wall should exceed the corresponding forces between the gas and a condensate layer; thus, the gas-wall accommodation coefficient should exceed the gas-condensate accommodation coefficient. Therefore, it should be conservative to use the value for the accommodation coefficient obtained previously ($\alpha = 0.77$). It then requires 4 collisions to reduce the molecular energy below the critical value. This then requires that $4A_0/A_S < 0.01$.

In general, since this condition can always be met, the losses will be dominated by the ratio A_0/A_C .

A further advantage of this approach is the reduced possibility of sputtering of the condensate layers. This is due to the initial collision for essentially all the incoming molecules being with a cold metal wall and not a condensate layer. The possibility for sputtering on subsequent collisions is also small because of the low average energy level of the molecules striking the condensate layer.

While the basic analysis has been made for a spherical configuration, it may be more convenient to use a cylindrical configuration. This change would not alter the results, since in general the inlet area is too small to maintain the pressure gradients that are required to prevent a nearly uniform distribution from being established.

F. Noncondensable Gases

A fraction of the ambient gas sample captured by the collector will be made up of gas species which are either noncondensable at the 20°K cryopump temperature or will have an unacceptably high solid vapor pressure. This fractional amount will constitute an inaccuracy in the determination of the ambient density by the proposed mass collection

principle. The three gases of concern, helium, hydrogen and neon, are present in small amounts in the homosphere where the various species are distributed according to a common number density-altitude profile due to general turbulent mixing. Above the mictopause, however, where the homosphere ends and the heterosphere starts, changes in the atmospheric composition occur as a result of gravitational separation and by interaction with incoming radiation. The gravitational separation tends to increase the relative percentage of the light gases in the atmosphere and thus potentially aggravates the noncondensable gas problem. Unfortunately, almost no data are available concerning the composition in the subject range of interest (140 to 280 km altitude); however, theoretical estimates can be used to arrive at approximate effects. If 100 km is conservatively used as the mictopause and the composition is calculated for the extreme case of 280 km altitude, helium is found to constitute 0.014 percent of the entering gas sample mass flux and hydrogen is 0.002 percent. Neon, being a heavier gas, varies by only a small amount from the homosphere percentage, i.e., 0.0012 percent. The presence of noncondensable gas species in the entering gas sample thus constitutes an extremely small error in the ambient density determination by mass collection.

IV. MEASUREMENT TECHNIQUE AND ACCURACY

A. Intermittent Collection

1. Minimum Collection Time

The minimum collection time may be set by the desired accuracy in measuring density variations as a function of altitude or by anticipated diurnal density variations. In either case, the optimum configuration of collector and pressure transducer should produce the maximum measurement pressure for a given collection time. From equation (2),

$$P_m = \rho_a \frac{A_{out} R_m T_m}{V_c + V_g}.$$

This can be expressed in terms of the important collector parameters as follows:

$$P_m = \frac{.9227 \rho_a R_m T_m ut (D_o/D_c)^2}{V_g^{1/3} (L_c/D_c)^{2/3}} (\beta), \quad (8)$$

where

$$\beta = \frac{(V_c/V_g)^{2/3}}{(1 + V_c/V_g)}.$$

The collector length-to-diameter ratio (L_c/D_c) and the inlet orifice-to-collector diameter ratio (D_o/D_c) are determined by requirements of capture coefficient; thus, the measuring pressure (P_m) is maximized by the function β . Maximizing β , we find that a collector-to-gage volume ratio of 2 will yield the maximum pressure, although volume ratios between 1 and 4 give results within 95 percent of the maximum.

This optimum pressure is plotted versus the collection time normalized by the orbital period in Figure 6. In this case, the collector-tube-to-aperture area ratio is taken as 10 with the collector $L/D = 5$. This geometry gives an estimated capture coefficient of 98 percent as discussed in the previous section. The most promising pressure transducer encountered in the study (MKS Baratron gage) has a full range pressure measurement capability of 1000 microns and a volume of 18 cm^3 . An evaluation of the minimum gage measurement pressure thus relates the minimum collection time and the measurement altitude.

To resolve the diurnal density variation, the collection time should not be greater than one-tenth of an orbit, i.e., $t/t_o < 0.1$. Available data indicate that the magnitude of this diurnal variation may be on the order of a factor of two in measured density. This represents a significantly greater density change than that encountered due to an orbital decay. Approximately 40 orbits would be required, for instance, to obtain this variation from strictly altitude change in the case of the S-IVB stage of the Saturn vehicle decaying from an initial 180 km circular orbit. Thus, the controlling time requirement is the diurnal density variation; this limits the collection time to not more than 0.1 orbit.

2. Altitude Range

The maximum altitude at which meaningful density determinations can be made is related to the minimum measurement pressure. If this minimum pressure is assumed to be 10 percent of the instrument's full range, i.e., approximately 100 microns, Figure 6 indicates a maximum measurement altitude on the order of 220 km due to insufficient pressure.

The low altitude limit is set by gas dynamic considerations rather than the measuring gage, since the assumption of free molecule flow at the collector inlet is basic to the determination of the swept ambient gas volume. The free molecule flow limitation is characterized by the diameter of the vehicle and the mean free path for collisions between free stream molecules and those emitted from the vehicle. Scattering of the free stream molecules by the emitted molecules begins to become significant, that is, greater than 10 percent, when the ratio of diameter to mean free path approaches unity. The ratio of free stream mean free path to the mean free path between emitted and free stream molecules at orbital velocities is about 12. Therefore, for a vehicle diameter of 6.6 meters, the required free stream mean free path is about 79 meters which corresponds to an altitude of 165 km. This lower limit can be reduced to 140 km by applying first-order corrections to the measurements to account for the scattering effects of the free stream. First-collision scattering calculations of the type developed by Wainwright and Rogers [3] and others can be made for mean free path lengths down to 1/4 of the 79 meter threshold. The design operational range of the instrument, then, is 220 km to 140 km, and spans a factor of approximately 17 in density.

3. Measurement Accuracy

The overall accuracy of the measurement system will depend upon the confidence which can be placed in the primary measurements of pressure, temperature, vehicle speed and altitude and in the evaluation of certain systematic effects, such as the collector capture coefficient, distortion of the free stream flow field by the vehicle, leaking of the measurement chamber, etc. All these factors are represented in the equation used to calculate the density.

$$\rho_a = K_L \frac{P_m}{R_m T_m} \frac{V_c + V_g}{u A_o t \phi}, \quad (9)$$

where ρ_a is the ambient density of the atmosphere, P_m and T_m are the measured pressure and temperature in the collector, R_m is the gas constant of the gas in the collector, K_L is a collector leak factor, $(V_c + V_g)/A_o$ is the ratio of collector and gage volume to collector aperture area, ϕ is the capture coefficient, u is the free stream velocity, and t is the collection time interval.

The collector pressure and temperature are the primary measurements, and their accuracy will depend upon the quality of all elements in the measurement chain from the transducer to the ground-based telemetry station. Attention is directed in this study to system

elements up to the telemetry encoder and transmitter with the view that the overall system accuracy up to this point will determine the quality of standard telemetry elements which can be justified. Mechanical diaphragm type pressure transducers in the 1000 micron pressure range are presently available which can produce 0.5 percent measurements. Deflection of the diaphragm is detected by variations in capacitance which is produced relative to a fixed surface. The transducers are sensitive to temperature gradients; but since the entire densitometer instrument will be conditioned and held at liquid nitrogen temperature, transducer temperature sensitivity should not pose a problem. The volume-to-aperture area ratio, $(V_c + V_g)/A_0$ has an uncertainty of 3 percent.

It is anticipated that the collector chamber temperature will be controlled rather than measured. Control would be achieved by regulating the pressure over boiling liquid nitrogen. At 100°K, a 7 percent tolerance in the regulated pressure yields only a 1 percent error in temperature. In addition to this advantage, boiling point control eliminates the need for one telemetry channel.

Determination of R_m , the gas constant of the collected gas at the measurement temperature, T_m , involves some estimate of atmospheric composition at the measurement altitude and an assumption that all decomposed molecules collected in the atmosphere will be recombined by the time of measurement in the chamber. The latter assumption is well founded because of the high collision frequency of the captured gas at the measurement pressure relative to the time required to evaporate the collected gas and measure.

The errors induced by uncertainty in composition depend upon the molecular weights of the components and the composition. If, for example, the concentrations of nitrogen and oxygen are considered with the concentration of oxygen equal to θ , the error in evaluating R_m relative to the uncertainty in θ is given by

$$\frac{dR/R}{d\theta/\theta} = \frac{1}{1 + \frac{M_N}{\theta(M_O - M_N)}} , \quad (10)$$

where M_N and M_O are the molecular weights of nitrogen and oxygen, respectively. It is seen that a 20 percent uncertainty in θ yields only a 0.55 percent error in R_m . Thus, a relatively crude estimate of oxygen-nitrogen composition will suffice to give a value for R_m whose accuracy is consistent with the other factors of the density determination.

The leak factor, K_L , is associated with the integrity of the pressure seal for the measurement chamber enclosing the collector during the warmup and measurement cycle. The only seal in the gas collector system is in the shutter over the inlet aperture. For the standard flight conditions associated with a 180 km orbit and assuming warmup and measurement time of the same order as the collection time interval, an uncertainty of 8×10^{-5} liter/sec in leak rate would yield an uncertainty in measured pressure of 1 percent. Leak rates of at least an order of magnitude higher could be tolerated provided it is known and repeatable to within 8×10^{-5} liter/sec. It is anticipated that a teflon O-ring type seal can be developed to meet these requirements. Tracking procedures are capable of providing measurements of vehicle velocity to within 0.1 percent. The shutter governing the collection time, t , would be controlled by a programmer which would govern all the functions of the instruments. It is estimated that the opening and closing time would be of the order of 0.5 sec with a repeatability of 0.05 sec. Thus, with a normal collection time of 500 sec, the accuracy of t should be 0.1 percent or better.

The last major item which must be known for the evaluation of density is the capture coefficient, ϕ . If reference is made to Section III on the collector design, it is seen that the cylindrical tube collector equipped with the proper aperture is capable of capture coefficients on the order of 98 percent. Thus, the fraction of swept molecules which are lost, i.e., the complement of ϕ , is approximately 2 percent.

Intermittent collection for the determination of ambient density by pressure transducer measurement thus has an uncertainty of approximately 8.2 percent up to the telemetry system which in itself has approximately a 1 percent uncertainty.

B. Continuous Collection

1. Maximum Collection Time

A resonating quartz crystal responds to changes in system mass, e.g., the deposition of a condensing gas, by a shift in the resonant frequency. The crystal can therefore be employed as a micro-balance, if other potential indeterminables are eliminated. Certain crystal cuts are highly sensitive to temperature; however, cuts can be made which eliminate this effect over the desired temperature range. From the work of Waters and Raynor [4] and Stephens [5 and 6], a $39^\circ 40'$ A-T cut has been found to be insensitive to temperature changes below 20°K . The sensitivity of the crystals in thickness shear resonance as a function of resonant frequency was presented in equation (3).

$$\Delta f = C \Delta m f_r^2$$

where

$$C = 2.26 \times 10^{-6}$$

$$\Delta f - \text{cps}$$

$$\Delta m - \text{gms/cm}^2$$

$$f_r - \text{cps.}$$

The crystal response becomes nonlinear when the frequency shift due to mass addition becomes approximately 1 percent of the resonant frequency. The allowable mass change for linear crystal response is thus

$$\Delta m_{\max} = \frac{4.42 \times 10^3}{f_r}. \quad (11)$$

Evaluating the system at 180 km altitude from available atmospheric property data then gives a maximum continuous collection time for linear response:

$$t_{\max} = \frac{10^{10}}{(A_o/A_c)f_r} \text{ secs,} \quad (12)$$

where

$$A_o = \text{aperture area}$$

$$A_c = \text{crystal area.}$$

An earlier discussion indicated the necessity of area ratio values, (A_c/A_o) , of approximately 100 to minimize measurement error due to escaping molecules; thus, the normalized maximum continuous collecting time becomes

$$\frac{t_{\max}}{t_o} = \frac{1.8 \times 10^8}{f_r}, \quad (13)$$

where again t_0 is one orbit period - in this case 5600 seconds. Crystals are available in the 1 to 10 megacycle range which are adequate for the orbit lives under consideration. The linear response range of operation is not an absolute limitation, of course, and calibration of the crystal response over a wider frequency shift range would extend the data-producing collection time. The disadvantage of this scheme would be the inconvenience of summing the accumulated mass in order to determine the changing crystal sensitivity during the flight.

2. Altitude Range

The maximum altitude at which continuous collection for density measurement with a quartz crystal can be used is related to the minimum measurable condensed mass change and the length of time between measurements. The frequency shift, equation (3), can be related more directly to collector parameters and the collection time by rewriting as follows:

$$\Delta f = C f_r^2 (\dot{m}/A_0) \frac{A_0}{A_c} \frac{t}{t_0} t_0$$

or

$$\Delta f = C f_r^2 (\rho_a u) \frac{A_0}{A_c} \frac{t}{t_0} t_0. \quad (14)$$

From earlier discussions certain restraints are imposed upon some of these parameters. It was established, for instance, that the area ratio, A_0/A_c , must be on the order of .01 for a high capture coefficient, and t/t_0 can be no larger than 0.1 in order to measure diurnal density variations. The orbital period, t_0 , is not greatly affected by orbit altitude nor is the vehicle velocity, u , which together with the ambient density, ρ_a , forms a product which is the entering mass flux per unit area, \dot{m}/A_0 . It is apparent then that the minimum measurable value of ambient density, ρ_a , is simply a function of the accuracy with which the frequency shift, Δf , can be measured. The percentage frequency shift for a given mass change is proportional to the basic crystal resonant frequency:

$$\frac{\Delta f}{f_r} = C \Delta m f_r. \quad (15)$$

Therefore, selection of high crystal frequency increases the measuring sensitivity, although as shown in the last section this implies a shorter continuous collection time before nonlinear crystal response occurs.

Since the frequency shift sensing and telemetry system has a limiting accuracy of approximately 1 percent, it is important that the total frequency shift be limited as much as possible in order to minimize inaccuracies in ρ_a . In the case of continuous collection, however, this total frequency shift may be on the order of 10,000 - 100,000 cps for a normal orbital lifetime. To reduce the magnitude of the shift, either the crystal must be thermally cycled to revaporize condensed mass between measuring points, thus returning the crystal to a zero frequency shift condition, or a beat frequency system must be employed in such a manner as to reduce the shift. The thermal cycle scheme introduces a complexity in the cooling system which is undesirable. On the other hand, the beat frequency technique increases the sophistication of the electronics sensing system, although in this particular application, the cooling system is by far the more difficult component system.

Smaller frequency shifts can be obtained by mixing the output of the measuring crystal with that of a variable reference oscillator. The resulting beat frequency is kept within a prescribed frequency range by driving the reference oscillator to new frequencies as the beat frequency reaches maximum set values. The reference frequency is varied by means of a frequency-voltage converter operating a voltage-controlled drive motor on the variable oscillator. For the particular flight orbits considered in this study, a converter providing a 0.5 to 4.5 volt DC signal corresponding to a 50 cps to 450 cps beat frequency is appropriate. This sensing system is shown schematically in Figure 7.

The maximum altitude at which the proposed instrument can measure density thus becomes a question of the desired accuracy of the measurement. The telemetry system results in a 5 cps uncertainty for the beat frequency system; thus, a frequency shift of 50 cps yields 10 percent uncertainty in the density determination. Equation (14) thus indicates the following minimum measurable densities as determined by the crystal resonant frequency and assuming the use of the aforementioned beat frequency system:

f_r	ρ	h
1 mc	$5 \times 10^{-9} \text{ kg/m}^3$	134 km
5 mc	$2 \times 10^{-10} \text{ kg/m}^3$	220 km
10 mc	$5 \times 10^{-11} \text{ kg/m}^3$	283 km

The low altitude measurement limitation can be imposed by the same gas dynamic condition which sets the limit for the intermittent system, or it may be determined by overloading of the crystal by the high mass flux at the lower altitudes. Based on the assumed flight vehicle, the lower altitude limit set by deviation from free-molecule flow conditions was found earlier to be 140 km. At this altitude, the maximum continuous collection time is

$$\frac{t_{\max}(140 \text{ km})}{t_0} = \frac{3.2 \times 10^7}{f_r} . \quad (16)$$

Thus, a 5 mc crystal would remain in the linear response regime for 6 orbits, and data could be obtained for continuing orbits. It must be concluded that mass flux is not the determining factor, and that the low altitude limit is 140 km, resulting from the vehicle size influence on the departure from the free molecular flow condition.

3. Measurement Accuracy

The overall accuracy of the continuous collection measurement system depends upon the factors represented in the equation used to calculate the ambient density by this technique:

$$\rho_a = \frac{\Delta f}{C f_r^2 u \phi(A_0/A_c) (t/t_0) t_0} . \quad (17)$$

The error in density determination due to the error in frequency shift measurement is $d \Delta f / \Delta f$; therefore, the magnitude of the error is determined not only by the frequency sensing equipment accuracy, $d \Delta f$, but also by the magnitude of the frequency shift itself. The uncertainty is thus influenced by the collection time for a particular measurement and by the orbit altitude. The frequency-to-voltage converter discussed previously is the only component in the best frequency sensing system up to the telemetry encoder which can introduce reading errors. This type of converter is a standard commercial component with 0.1 percent full scale accuracy. There will, however, be errors on the order of 1 percent in the telemetry of the beat frequency generated voltage signal.

Since the maximum beat frequency is a set value, the inaccuracy cannot be less than 1 percent and can be more for short measurement intervals or for higher altitudes which result in less than full scale frequency shifts. Evaluation of the frequency shift from

equation (17) with a 10 mc crystal and an orbit altitude of 180 km indicates that the full scale shift of 500 cps will occur in approximately 1/12 of an orbit which is less than the maximum allowable time. Thus, at 180 km which has been considered to be the nominal orbital altitude in this study, the frequency shift has an uncertainty of 1 percent.

In this type of sensing system, the actual value of the reference oscillator frequency is immaterial, and it is only important that the stability of the frequency during a particular measurement time period be assured. Temperature control of those standard oscillators results in extreme stability, and frequency shifts in the reference oscillator will be negligible.

As previously discussed, tracking procedures provide a measurement of vehicle velocity to within 0.1 percent. The fraction of swept molecules lost due to non-unity capture coefficient is approximately 2 percent.

The inlet aperture to crystal area ratio, A_0/A_c , has an uncertainty of 3 percent. The crystal's resonant frequency determination, as well as the collection time between measurements, contributes a negligible uncertainty.

Continuous collection for the determination of ambient density by a cryogenically cooled quartz crystal micro-balance thus has an overall system measurement uncertainty of approximately 6.1 percent, including telemetry error.

V. COOLANT SYSTEM

A. Intermittent Collection

1. Cooling Scheme

The component elements of the intermittent collection system are shown schematically in Figure 8. The major elements are the collector, the pressure transducer, the aperture shutter, the two thermal switches, the heat transfer rod, a liquid nitrogen source, and the liquid helium reservoir. A typical measurement cycle begins with the cooldown of the collector to liquid helium temperature by closure of the transfer rod thermal switch. During this cooldown, the aperture shutter is closed and the collector is isolated from the liquid nitrogen source. After collector cooldown has been achieved, the shutter will open for the prescribed collection time, permitting a known volume of ambient air to be captured. The next step is the vaporization of the condensed air sample and pressure measurement by the transducer. This is accomplished by

opening the transfer rod thermal switch and bringing the collector into contact with the liquid nitrogen source thereby warming the collector to 100°K. The shutter is closed and sealed against the inlet aperture during the warmup to liquid nitrogen temperature. After warmup is achieved and the pressure measured, the shutter is opened, venting the collected gas out to the atmosphere and reducing the residual pressure to a negligible level. The collector is then ready for another liquid helium cooldown and sample collection.

2. Refrigeration Requirements

The quantity of liquid helium required to accomplish the measurement mission depends upon the requirements per measurement cycle and the total number of cycles in the mission. A frequency of 10 measurements per orbit was previously found to be required to resolve diurnal density variations. The descent from 180 km to 140 km will require 55 orbits of the assumed flight vehicle. Therefore, a maximum of 550 measurements would undoubtedly suffice for both altitude variation measurement and the diurnal variation. Therefore, the number of measurement cycles could be considerably reduced if the operation of the aperture shutter is controllable.

(a) Cooldown Requirement

The liquid helium volume requirement for collector cooldown is related to the collector heat capacity and a specific liquid requirement as follows:

$$\frac{m_{\text{He}}}{\rho_{\text{He}}} = \frac{\delta_c \rho_c A_c \xi}{\rho_{\text{He}}} = \frac{\delta_c \rho_c \xi}{\rho_{\text{He}}} (V_g)^{2/3} (V_c/V_g)^{2/3} (A_c/V_c)^{2/3}, \quad (18)$$

where

δ = collector wall thickness

ρ_c = collector density

ρ_{He} = liquid helium density

A_c = total collector area

ξ = specific liquid requirement.

From this equation, the collector L/D for the minimum value of $(A_c/V_c)^{2/3}$ can be found which will lead to the minimum helium requirement. Solution in this manner results in an L/D = 1 collector as the optimum configuration. Previous discussions indicated, however, that an L/D = 5 cylindrical collector was required in order to achieve near-unity capture coefficients. Evaluating this configuration as compared to the optimum configuration indicates only a 15 percent penalty in the helium requirement for an L/D = 5 collector.

The specific liquid requirement, ξ , is the number of grams of liquid helium required to cool a gram of the collector material over a specified temperature interval, and has been analyzed by Jacobs [7]. In this particular application, copper would probably be used for the collector walls because of high thermal conductivity characteristics at low temperatures. A value of $\xi = 0.5$ applies to the cooling of 100°K copper to liquid helium temperature, if only the heat of vaporization is available. Use of a boiloff vent system which makes use of the gaseous helium's heat capacity in the cooldown would reduce ξ to 0.03. The more conservative figure will be used in the following calculations.

The optimum collector to gage volume ratio, V_c/V_g , was earlier found to be 2 and the gage volume is on the order of 18 cm³. For a collector wall thickness of $\delta_c = 0.005$ cm, the required liquid helium volume for cooldown is thus calculated to be 12.4 cm³ for each cycle.

(b) Condensed Gas Requirement

During the measurement cycle, the collector walls and transfer rod transfer the heat load associated with the condensation of the mass of entering free stream air to the liquid helium where boiloff will balance the heat load. The energy to be removed is essentially the kinetic energy of the entering air and can be related to the liquid helium volume requirement as follows:

$$\frac{m_{He}}{\rho_{He}} = \frac{\frac{1}{2} u^3 \frac{A_o}{A_c} A_c \frac{t}{t_o} t_o \rho_a}{\rho_c H_v}, \quad (19)$$

where

H_v = helium heat of vaporization.

Using $t/t_0 = 0.1$ for the sampling time and the optimum collector to gage volume ratio,

$$\frac{m_{\text{He}}}{\rho_{\text{He}}} = 3.71 \times 10^{12} \rho_a. \quad (20)$$

Evaluation at a nominal 180 km altitude results in a requirement of 2.22 cm^3 of liquid helium for each measurement cycle. This volume requirement is directly proportional to the ambient density and thus is easily evaluated as a function of altitude.

(c) Helium Reservoir

The requirement of $14.6 \text{ cm}^3/\text{cycle}$ of liquid helium for a maximum of 550 cycles implies a helium reservoir volume of 8 liters. In addition to the heat load associated with the gas collection process, there are heat leaks through the insulation of the reservoir. Assuming the use of multilayer insulation and 80°K surrounding temperature results in a requirement of $0.2 \text{ cm}^3/\text{cycle}$ of liquid helium. To the total cycle requirements should be added an additional 16 cm^3 of liquid helium to account for reservoir insulation losses during a 12-hour prelaunch period. The total amount of helium required for 550 measurement cycles plus a 12-hour hold period is 8166 cm^3 which implies a 10-inch diameter spherical reservoir.

B. Continuous Collection

1. Coolant Scheme

Using the quartz crystal sensor as a continuous cryopump for the entering mass flux reduces the refrigeration requirements considerably compared to the intermittent collection system, inasmuch as there is no need for a thermal cycling phase in the coolant system, thus eliminating a major heat load.

The reduced level of heat load makes possible the use of a precooled metal mass acting as a heat sink for a simple source of refrigeration.* The coolant system, schematically shown in Figure 9,

* An alternate cooling scheme by hydrogen sublimation is presented in Appendix D.

consists of the crystal heat sink mass (nominally at liquid helium temperature) in an insulated container, a conduction path from the heat sink to the crystal, and a gas collector constructed such that the walls act as a heat sink at a temperature near 100°K. The two heat sinks are pre-cooled before flight with liquid helium and liquid nitrogen by means of coolant coils integral to the heat sink masses. The collecting period is initiated at the desired altitude by permanently removing an aperture cap which has previously maintained vacuum conditions in the collector, thus keeping the heat load to a minimum during prelaunch holds and the initial portion of the flight. The heat sinks slowly rise in temperature during the measurement period. Accurate measurement conditions are maintained, however, as long as the crystal temperature remains at a level which results in condensate vapor pressures at least an order of magnitude less than the gas sample pressure, and the collector walls remain below a level which would produce an unacceptable radiation heat load to the crystal or which would not reduce sufficiently the temperature of incoming gas molecules. The analyses in the following sections result in a crystal heat sink of 55 cm³ of lead and a collector wall heat sink of 113 cm³ of aluminum.

2. Refrigeration Requirements

A hypothetical mission will be used in this analysis of the required refrigeration system, consisting of an unattended 12-hour hold period of the vehicle before launch followed by a 55-orbit flight.

(a) Crystal Sensor

(1) Radiation Heat Load - The crystal receives a radiation heat load from the collector walls not only during the measurement period but also during any unattended prelaunch hold periods. The design of the crystal heat sink mass must take into account, then, the operational problems involved in large vehicle launches.

The collector wall being a heat sink will be varying in temperature during the flight; however, a conservative heat load is obtained if a wall temperature of 90°K is used in the calculation. The crystal can conservatively be considered to have an absorptivity of unity and the collector wall will be polished to an emissivity of 0.1.

The maximum available crystal diameter is approximately 2.2 cm; therefore, $A_c = 3.95 \text{ cm}^2$, and from the radiation heat transfer equation,

$$Q_r = (5.67 \times 10^{-12}) \epsilon A_c (T_w^4 - T_c^4) \quad (21)$$

and

$$Q_r = 1 \text{ milliwatt.}$$

(2) Gas Condensation Heat Load - The entering mass flux is reduced in temperature by the cold collector walls before encountering the crystal. Assuming the gas temperature is reduced to 100°K, the energy removal required, Δh , for condensation on the crystal is 83 cal/gm.

Using an altitude of 140 km for a conservative mass flux,

$$\dot{m}/A_0 = 26.5 \times 10^{-7} \text{ gm/sec} - \text{cm}^2.$$

The condensation heat load, using the fact that $A_c/A_0 = 100$, is then

$$Q_{\text{cond}} = (\Delta h) (\dot{m}/A_0) A_0 = 0.037 \text{ milliwatts.}$$

(3) Crystal Temperature Gradient - The equation for the temperature gradient in a flat conducting disc with a uniformly imposed heat load is

$$T_r - T_R = q \frac{(R^2 - r^2)}{4k\delta}, \quad (22)$$

where

q = heat load

k = thermal conductivity of disc

δ = disc thickness

R = edge radius

r = local radius.

The total imposed heat load due to radiation and gas conduction is

$$q = 2.6 \times 10^{-1} \text{ milliwatts/cm}^2.$$

Therefore, for a 0.015 cm thick quartz crystal ($k = 5 \text{ watts/cm}^\circ\text{K}$), the maximum temperature difference caused by the imposed heat load is $\Delta T = 0.005^\circ\text{K}$.

(4) Crystal Heat Sink - The material used in the heat sink should have a high specific heat in the applicable range of temperature to minimize heat sink weight, as well as a high density which will tend to minimize the displaced onboard volume. Lead is an appropriate heat sink material on this basis, and the following equation can be used to calculate the required mass of metal required for a given time interval:

$$m = \frac{Q \int dt}{\int c_p(T) dT} \quad (23)$$

The allowable heat sink temperature rise is determined by the criterion that the condensate vapor pressure should be an order of magnitude less than the collector chamber pressure for negligible error in condensed mass determination. With an area ratio $A_c/A_o = 100$, and with a speed ratio of approximately $S = 10$, the crystal has approximately ten times the volumetric pumping speed of the inlet aperture. The collector pressure during measurement will therefore be approximately 1/10 the ambient pressure. Using the condensate vapor pressure criterion thus results in a maximum allowable crystal temperature of 23.5°K. With the allowable $\Delta T = 18.5^\circ\text{K}$, solution of equation (23) results in a lead sink mass of 0.68 kg for the nominal mission described at the beginning of this section, which has a time interval of $t = 2.57 \times 10^5$ seconds. The required heat sink volume is 55 cm³.

The heat sink mass and cold vacuum container will be highly polished to minimize the radiation heat load to the heat sink itself, and the cold mass will be supported within the container by means of thin stainless steel tension wires providing a negligible heat leak.

(b) Collector Wall

(1) Insulation Heat Leak - In order for the collector wall to function efficiently as a heat sink, it must be insulated from the surrounding vehicle structure which is nominally at 300°K temperature. This is most conveniently accomplished by the use of multilayer aluminized mylar sheets, i.e., superinsulation. The heat transfer through this insulation is by both conduction and radiation, and is commonly expressed as follows:

$$Q = (5.67 \times 10^{-12}) \beta (T_{300^\circ\text{K}}^4 - T_s^4) A_s \quad (24)$$

where $\beta = 0.002$ for optimum superinsulation installation.

From the earlier discussion of capture coefficient criteria, the collector wall area, A_s , was related to the inlet aperture area, A_o , by the number of collisions required to reduce the incoming molecule temperature below a critical level, and to allow only 1 percent of the molecules to escape before being cryopumped. On this basis,

$$A_s > 400A_o.$$

For the aforementioned crystal, i.e., $A_c = 4 \text{ cm}^2$, this criterion would imply $A_s > 16 \text{ cm}^2$. In this study a larger collector has been considered in order to reduce the escaping molecular fraction below 1 percent and to arrive at a reasonable prototype design which groups all components, including the crystal heat sink mass, into a neatly packaged unit. A collector of 3.2 cm diameter by 8.9 cm length is therefore selected for the prototype design. This collector has a wall area of 88.8 cm^2 .

On the basis of this collector geometry, the collector wall heat load due to superinsulation heat leak is

$$Q_{\text{Ins}} = 8 \text{ milliwatts.}$$

(2) Gas Cooling Heat Load - The collector wall must cool the incoming mass flux to approximately 100°K before the gas molecules strike the crystal. The amount of energy which the wall must remove is essentially the kinetic energy of the incoming stream. Evaluation at 140 km altitude gives a conservative value of this energy removal requirement.

$$Q/A_o = \frac{1}{2} \rho u^3 = 84.5 \text{ milliwatts/cm}^2 \quad (25)$$

and

$$Q_{\text{cool}} = 3.38 \text{ milliwatts.}$$

(3) Collector Wall Heat Sink - The collector wall must serve not only as a heat sink but also structurally as a vacuum chamber containing the crystal sensor and the crystal heat sink. Aluminum is a more desirable metal in this application than the lead used in the crystal

heat sink, not only because of structural characteristics but also because of aluminum's greater specific heat in the desired temperature range, i.e., 70°K to 100°K.

For the total collector wall heat load of 11.38 milliwatts, equation (23) indicates that 0.31 kg of aluminum is required to maintain the wall temperature below 100°K during the assumed mission. The required metal volume is 113 cm³.

VI. SUMMARY DESCRIPTION OF RECOMMENDED SYSTEM

On the basis of the greater sensitivity of the crystal sensor, the simpler coolant system, compared to those connected with the intermittent method, and the fact that an inlet shutter is not required, the continuous collection system is deemed the most promising instrument for prototype development. All major components of this system have been conservatively analyzed for an assumed flight, and reliable density measurements can be expected with an overall error (including telemetry) of only 6 percent. A summary description of the system follows.

The densitometer consists of these major components:

- (1) A cylindrical orifice collector with a capture coefficient of 98 percent.
- (2) A cooled piezoelectric crystal which responds to mass addition from cryopumping with a frequency shift.
- (3) A measuring system consisting of a variable frequency oscillator and a beat frequency-to-voltage converter.
- (4) A refrigeration system consisting of two heat sinks, one of lead to cool the crystal to a temperature not higher than 23.5°K, and the other of aluminum which makes up the collector body and keeps itself at a temperature no higher than 100°K.

Figure 9 shows these components, and Figure 7 depicts the measurement scheme. Aside from electric power and telemetry, the densitometer system can operate independently of the vehicle. Vacuum and temperature conditioning of the system would be achieved on the ground either in a fixed or a mobile laboratory with relatively simple equipment requirements. Once conditioned and inserted into the vehicle, the system can withstand a hold of at least 12 hours without attention or umbilical connection.

Space, weight, power and telemetry requirements onboard a vehicle are estimated as follows:

(1) Space

Densitometer	650 cm ³
Electronics	15,000 cm ³

(2) Weight

Densitometer	1.4 kg
Electronics	4.5 kg

(3) Power - 30 watts at 28 volt DC.

(4) Control Signals and Telemetry

One control signal from onboard programmer to eject aperture cap.

Four telemetry channels:

- a. 0-5 volt DC
- b. monitor variable oscillator setting
- c. lead heat sink temperature
- d. aluminum heat sink temperature.

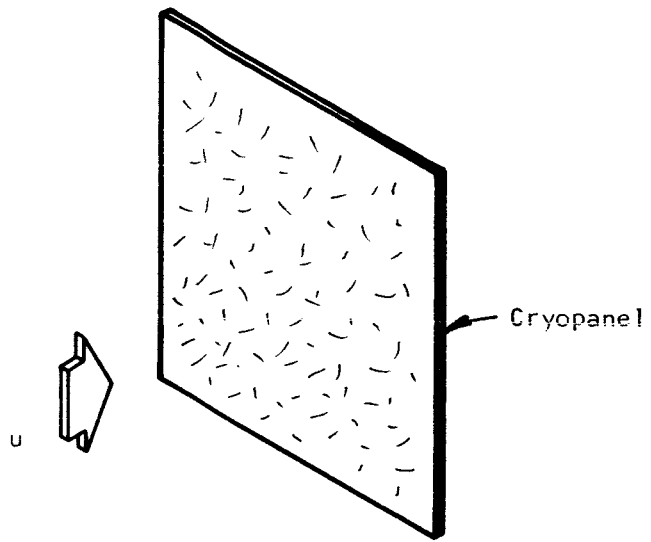


Figure 1. Cryopanel Normal to the Airstream

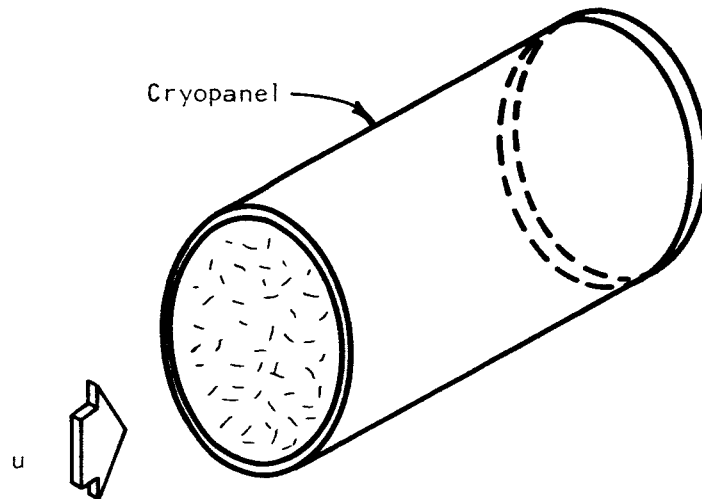


Figure 2. Cylindrical Cryopanel Aligned with Airstream

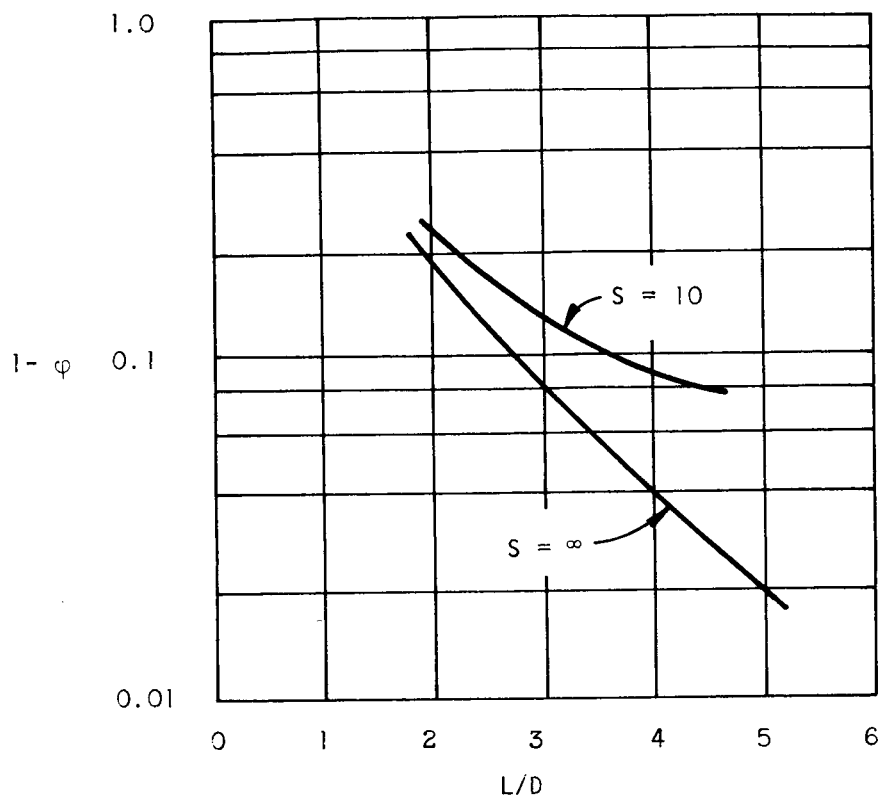


Figure 3. Effect of L/D and Speed Ratio

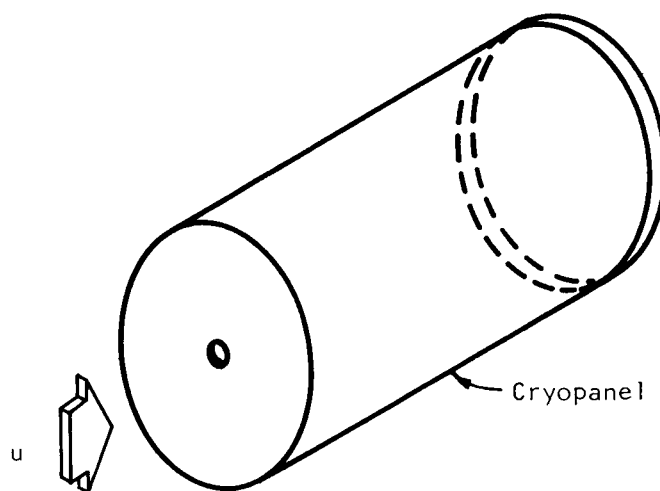


Figure 4. Cylindrical Cryopanel with Reduced Inlet Area

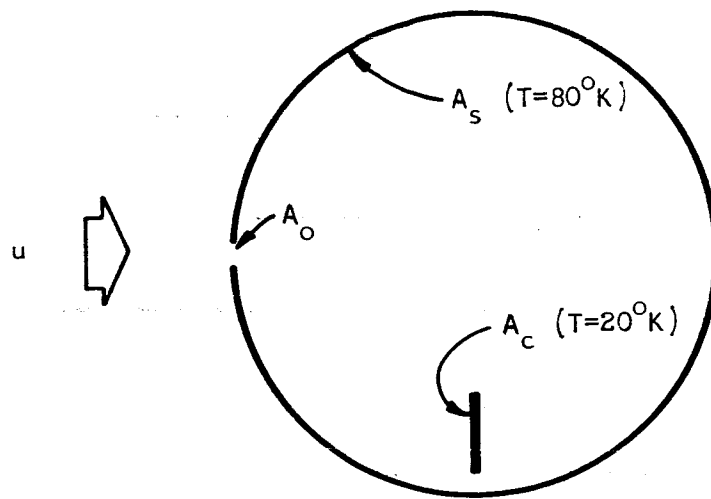


Figure 5. General Collector Configuration

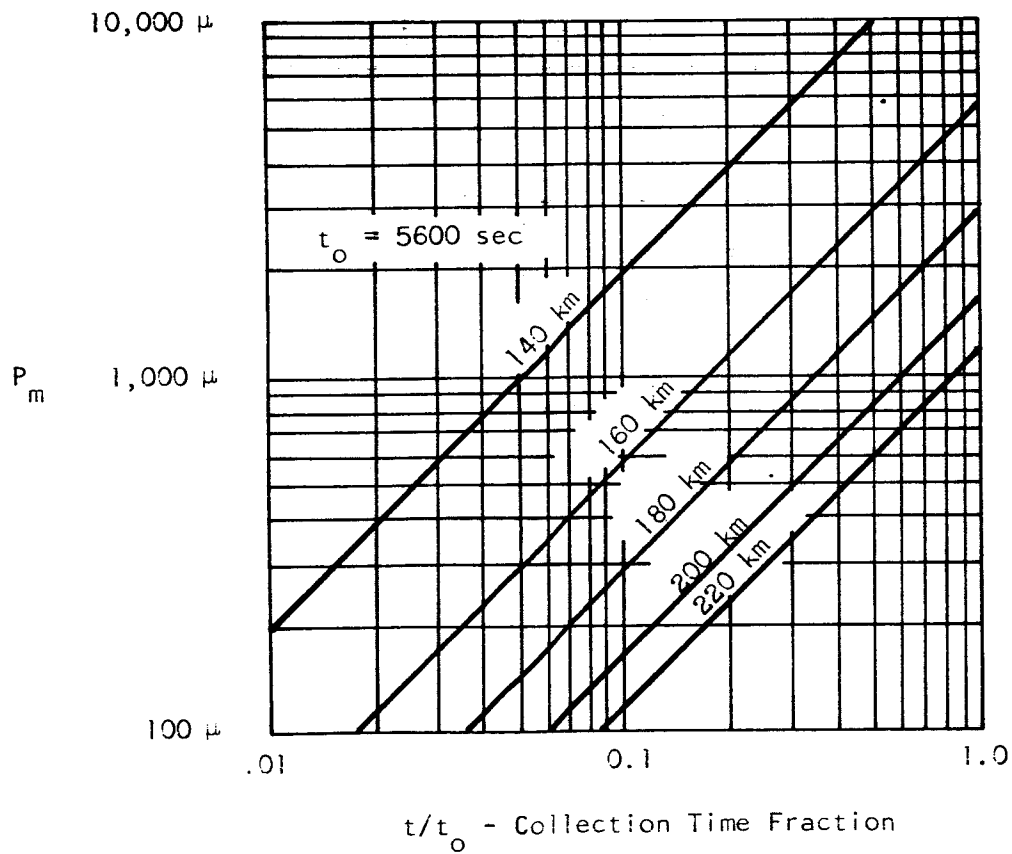


Figure 6. Measurement Pressure vs Collection Time Fraction

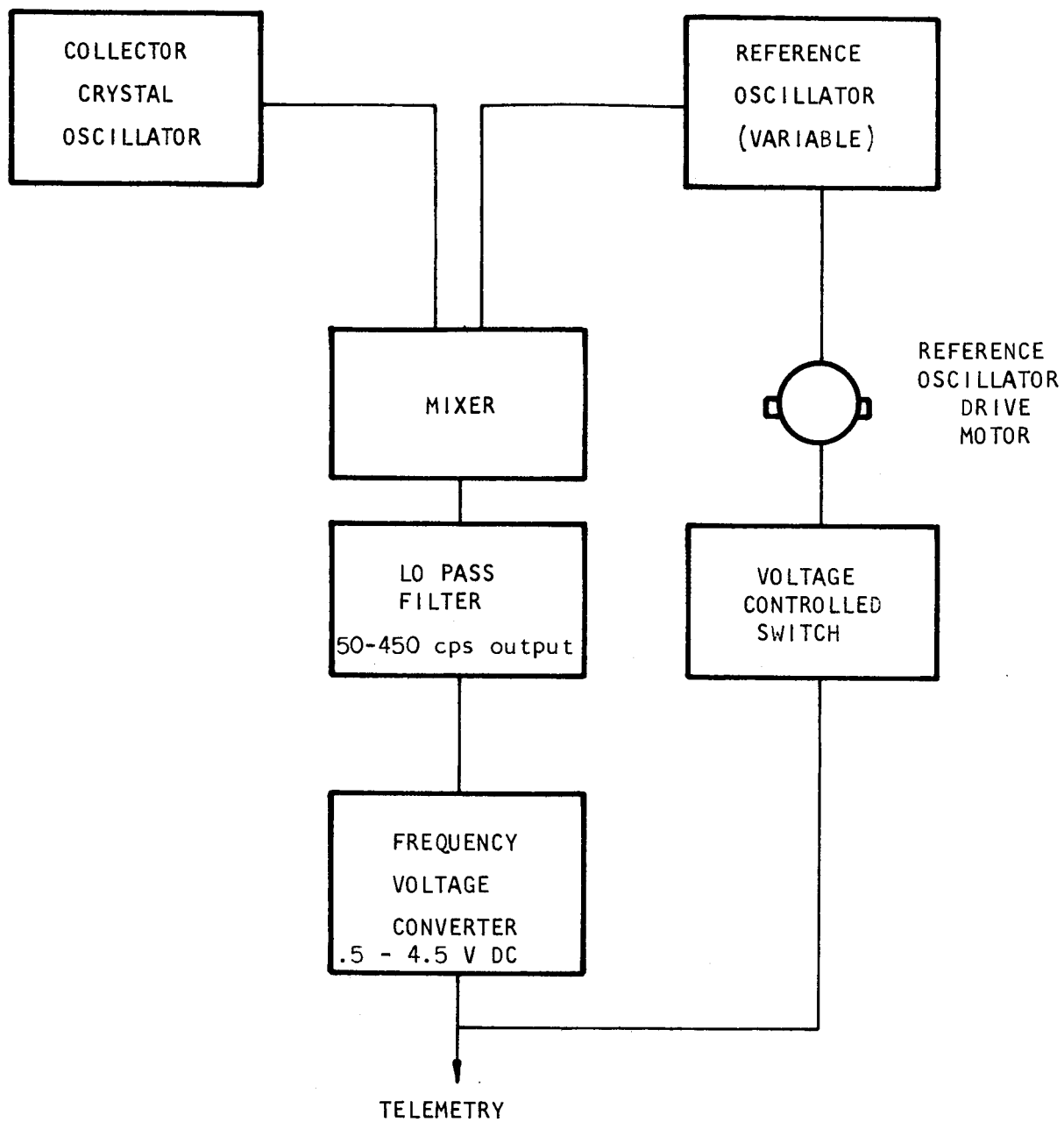


Figure 7. Crystal Sensor Frequency Shift Measurement System

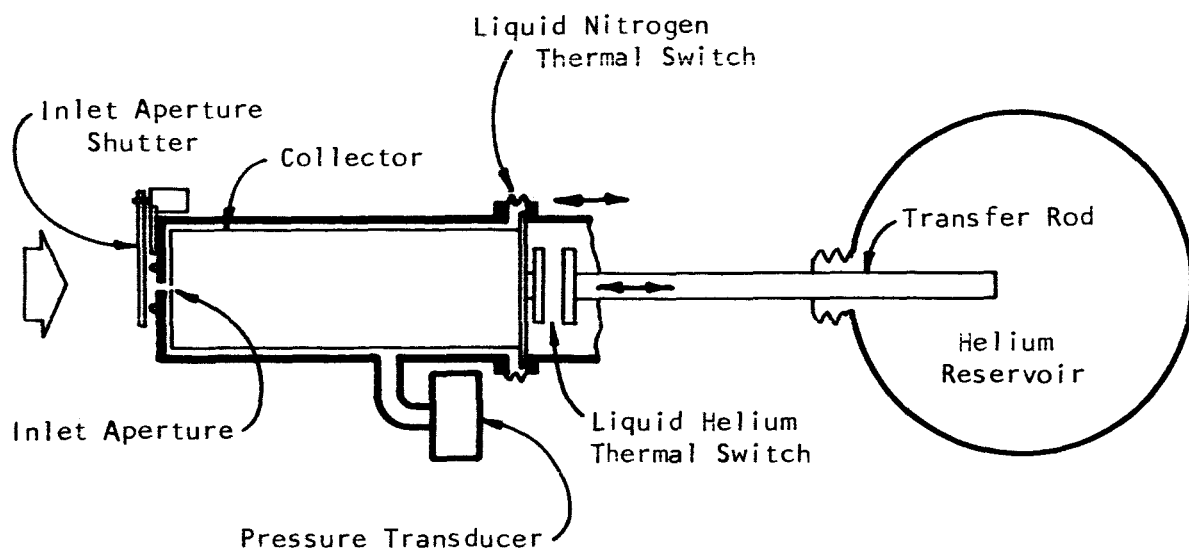


Figure 8. Intermittent Collector

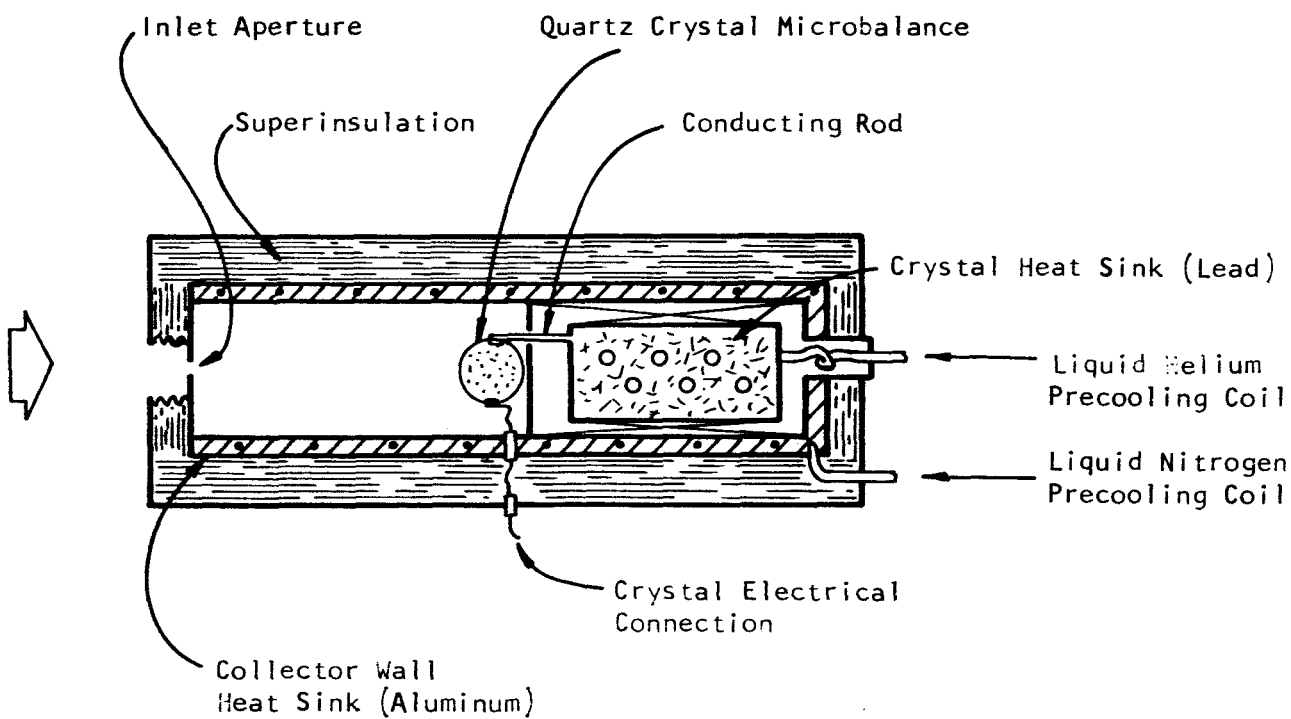


Figure 9. Continuous Collector

APPENDIX A

Capture Coefficient

During the start of the collection process, the incident molecules will strike a cryopanel that will probably be covered with layers of absorbed gases. As the collection process continues, a condensate layer will form, and the incident molecules will impinge upon the condensate layer. In principle, it is necessary to estimate the sticking coefficient for the incident gas impinging on these two types of surfaces, but in practice it is expected that only the collisions of the molecules on the condensate will be important. Since the incident gas is air with a composition comparable to the sea level condition, the important gases are nitrogen and oxygen.

No experimental data have been found corresponding to a high velocity directed flow impinging on a cryopump. The available sticking coefficient data is limited to flows with $S = 0$ and temperature below 400°K. Furthermore, investigators do not seem to be in agreement on the values of sticking coefficient. Wang et al. [8] found that the sticking coefficient increases as the thickness of the condensate layer increases. This increase ceased after a layer corresponding to about 10^4 monolayers was deposited. This suggests that the collector plate sticking coefficient would vary with the thickness of the condensate layer; however, Buffham et al. [9] using what seems to be a comparable experimental arrangement found no variation of sticking coefficient with condensate layer thickness. There is also a lack of agreement concerning the level of the sticking coefficient. Dawson [10] presents the results of a large number of tests that determined the variation of sticking coefficient with both cryopump temperatures and temperatures of the impinging gas. His sticking coefficients are significantly lower than the values reported by Buffham et al. [9], Bachler et al. [11] and Stickney and Dayton [12]. The experimental data are considered to be of limited value for two reasons: (1) the data do not cover the range of test conditions required, and (2) the data do not appear to be consistent among different investigations. In order to apply these data to the present analysis, theoretical methods must be used as a guide for extrapolation.

The theoretical investigations of the sticking coefficient have generally been limited to considerations of the one-dimensional model consisting of a monatomic molecule colliding with a chain of elastically coupled lattice molecules. Since these correspond to normal collisions, the results might be suitable for the highly directed flow that exists in the present investigation. One objection to this approach is the use of the highly organized linear oscillator lattice for a condensate layer that appears to have many voids and defects, Roder [13]. Another

objection is the fact that the collision model is only correct for an infinite speed ratio, while the speed ratio for a 180 km orbit is about 10. Although the random energy is small compared to the directed energy ($\sim 1/100$), the random energy is comparable to the heat of vaporization of nitrogen and oxygen so the condensation process may be influenced by the finite speed ratio.

Another theoretical approach has been considered by Buffham et al. [9]. They assumed that the gas arrived at the cryopump with a Maxwellian velocity distribution ($S = 0$) and all the molecules with an energy level below the critical energy level (E_c) were captured. The sticking coefficient was then obtained from

$$1 - \sigma = \left(1 + \frac{E_c}{RT}\right) \exp - (E_c/RT) \quad (A-1)$$

where

T = temperature of the surrounding gas.

Since no estimate was made for the value of the critical energy, it must be obtained from experiments. Figure A-1 is a plot of $1 - \sigma$ vs $1/T$ for a range of values of the parameter E_c .

Included are data points for nitrogen. The data of Dawson [10] indicate that the critical energy level is about 1500 cal/mole which is comparable to the heat of vaporization. The other data include values in excess of 4000 cal/mole. Since most experiments were only accurate to 1 or 25 percent, there is considerable uncertainty in the critical energy to be associated with the sticking coefficients of nearly unity. This could be more readily resolved with data obtained at a higher gas temperature.

From Figure A-1 it may be assumed that Dawson's data represent a lower limit of $E_c \approx E_b$, where E_b is the energy required to remove a molecule from the surface of the condensate. Since a prohibitive experimental accuracy would be required to set an upper limit on E_c using room temperature nitrogen, it is necessary to use a theoretical approach to estimate the upper limit.

McCarroll and Ehrlich [14] used the one-dimensional lattice to estimate E_c/E_b (see Figure A-2). They found that, for equal molecular weights, the energy ratio E_c/E_b varied with the spring constant ratio, K_c/K_k . K_c is the spring constant for the elastic coupling between the incident molecule and the lattice molecule, while K_k is the spring constant between the lattice molecules. If the masses and the spring constants were the same, they found that $E_c/E_b \approx 25$.

Only as K_c/K_k approaches 0.2 does the energy ratio approach unity which is the value obtained from Dawson's data. Since it is not known why this low value of K_c/K_k should exist, it appears that the energy ratio E_c/E_b can only be assumed to fall between 1 and 25.

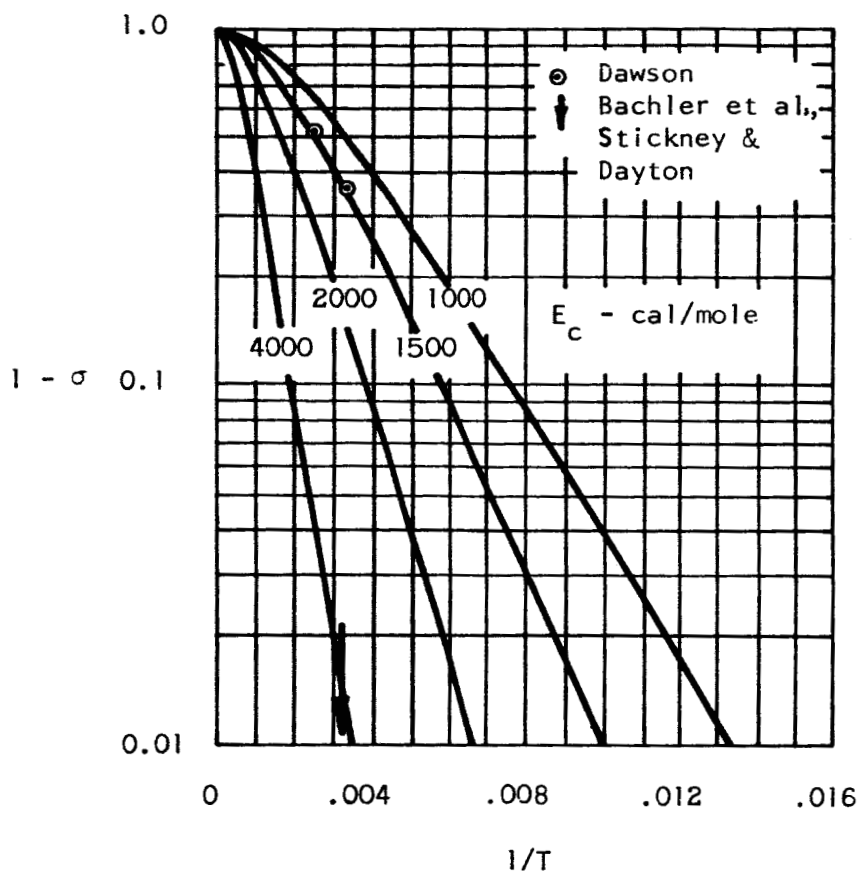


Figure A-1. Variations of Sticking Coefficient with Temperature

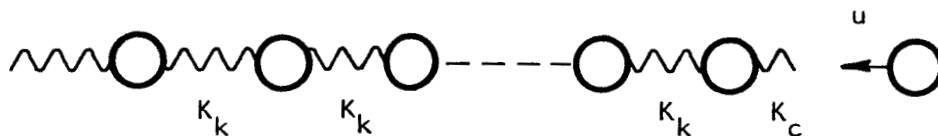


Figure A-2. One-Dimensional Model of Surface Interaction

APPENDIX B

Accommodation Coefficient

Since the energy level of the incoming molecules is about two orders of magnitude greater than the heat of sublimation while the critical energy for condensation is about the same order of magnitude as the heat of sublimation, it is clear that the incoming molecules must be cooled by successive collisions with the cold wall before condensation can occur. The number of collisions required will depend upon the accommodation coefficient.

$$\alpha = \frac{E_i - E_{\text{off}}}{E_i - E_{\text{wall}}} . \quad (\text{B-1})$$

The accommodation coefficient varies with such parameters as

- (1) gas species
- (2) wall species
- (3) gas temperature
- (4) wall temperatures
- (5) contamination of the wall surface.

There are no experimental data on the accommodation coefficient for high velocity, highly directional air impinging on a cryogenic surface which is covered with a layer of condensate.

Some limited data were obtained by Mayer et al. [15] using a cold plate normal to a supersonic stream. Since the flow was not free molecular relative to the plate, the temperature of the incident gas was lower than the stagnation temperature, and the data are not applicable to the present analysis.

In general, molecular beam data are not suitable since they have been obtained at relatively low energy levels and with no condensate layer.

Theoretical results often suggest the hard sphere approximation for high energy levels.

$$\alpha = \frac{4 (M_1 M_2)}{(M_1 + M_2)^2} \quad (\text{B-2})$$

where

M = molecular weight.

Unfortunately, this simple approximation is of questionable value if the molecular weight of the gas is equal to that of the solid, since it implies complete accommodation. The approach of Oman et al. [16] would undoubtedly be useful, but their results have not included the case where $M_1 = M_2$.

Rogers [17] did include the case of $M_1 = M_2$ in his investigations using an analog computer, but since his "wall" consisted of a single linear oscillator, it is questionable whether the results are quantitative. Other investigations have found that the effects of the collision penetrate into the wall for several molecular diameters during the time required for the collision to be completed. McCarroll and Ehrlich [14] have included calculations of the accommodation coefficient for $M_1 = M_2$ over a range of K_c/K_k (see Figure B-1).

Using the results of Appendix A, it is assumed that $E_c = B_d$ and $K_c/K_k = 0.2$; therefore, from Figure B-1, it appears that $\alpha = 0.77$ should be conservative.

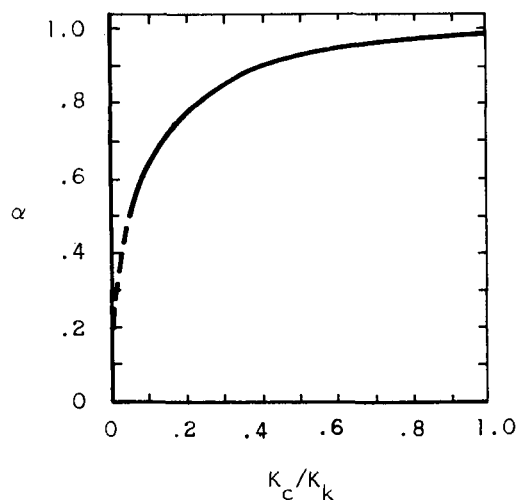


Figure B-1. Accommodation Coefficient Variation

APPENDIX C

Sputtering

When high velocity molecules or ions impinge on the surface of a target, they may cause some of the target material to be ejected or sputtered. This sputtering process is discussed quantitatively in terms of the yield which is defined as the ratio of the rate of sputtering of target molecules to the rate of incidence of energetic molecules or ions. The yield depends on the energy of the incident molecules, the binding energy of the target molecules, the angle of incidence and the atomic weights.

It has generally been found that molecules or ions which are traveling at satellite velocities do not cause measurable sputtering on metals; thus, there should be no erosion of the basic condenser surface during the collection cycle. There is still the possibility that the incident molecules will cause sputtering of the condensate layer. This possibility is due to relatively low binding energy of the condensate layer when compared to that of the typical metal.

Since no data were found on the self-sputtering of condensed nitrogen or oxygen, it was necessary to estimate the self-sputtering yield from the correlation of available data.

From a comparison of the sputtering of metals by noble gas ions, it was found that the mass of the incident ion was not a dominant factor if the yield was low. Therefore, a crude correlation was made using the data of Stuart [18] for argon ions on various metals. The correlation is presented in Figure C-1, which is a plot of yield vs the ratio of the energy of the incident ion to the heat of sublimation (E_i/E_b). The plot shows that the data correlate within an order of magnitude. Assuming that nitrogen has a similar self-sputtering yield, and noting that $E_i/E_b \approx 9/0.07 = 130$, it appears that the yield will be about 1. If this is correct, each incident molecule will sputter one molecule from the condensate layer. After the first collision, the energy level of the incident molecule is about $(1 - \alpha) E_c$; therefore, if $\alpha = 0.77$, the energy ratio E_i/E_b is about 30. Since the sputtering associated with this energy ratio is small compared to the uncertainty in the initial sputtering yield, any sputtering after the initial collision can be neglected.

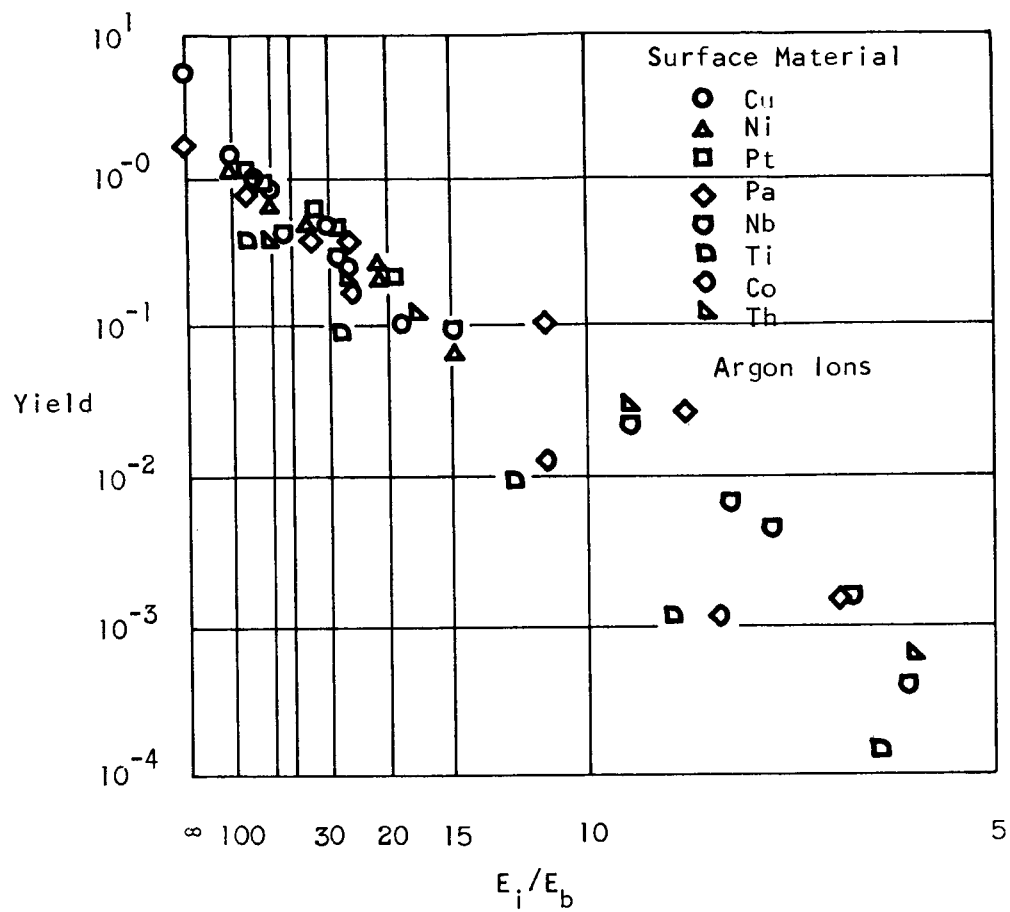


Figure C-1. Yield vs Energy Ratio

APPENDIX D

Refrigeration by Hydrogen Sublimation

A refrigeration system using the sublimation of solid hydrogen as the heat removal mechanism could be considered for cooling the crystal and the collector walls. This concept involves the relationship between the equilibrium vapor pressure of a substance and the substance temperature. A heat load impressed upon the substance can be removed from the system under constant temperature conditions if the substance sublimates and the evolved vapor is removed from the system at a rate which maintains a constant equilibrium vapor pressure. The heat removal capacity of such a technique is equivalent to the heat of sublimation of the substance which is equal to the sum of the heat of fusion and the heat of vaporization at the particular temperature of interest. A survey of candidate substances for such a scheme indicates that only solid phase neon and hydrogen meet the primary requirement of solid phase temperature near 20°K at readily controllable vapor pressure, e.g., greater than 1 torr (Figure D-1). The heat of sublimation of hydrogen (at 13.95°K) is

$$\Delta H_{s, H_2} = 125 \text{ cal/gm} \quad (D-1)$$

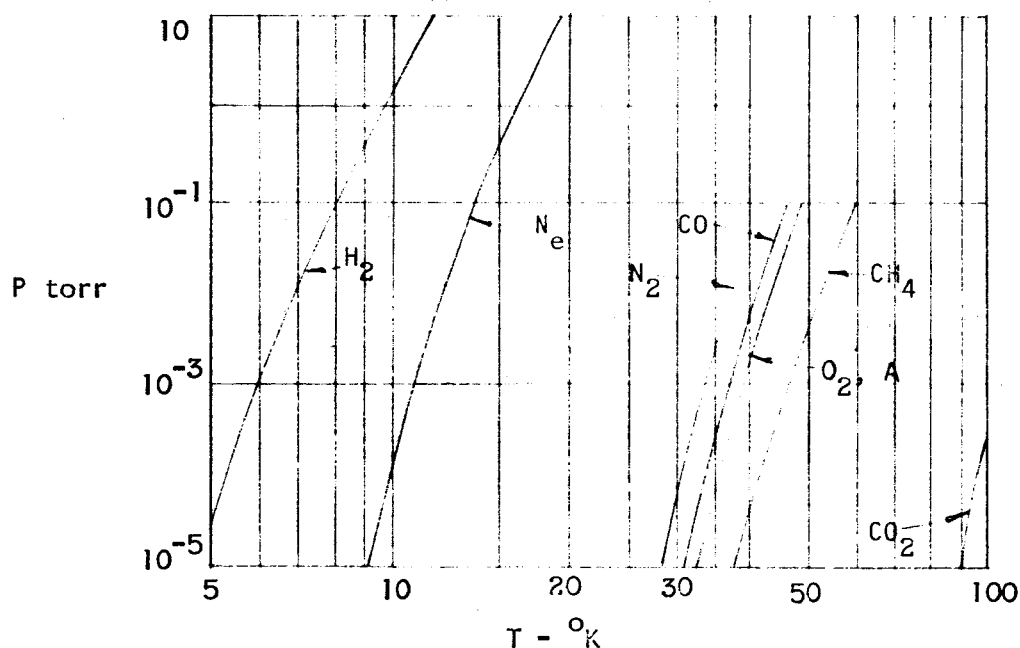


Figure D-1. Solid Phase Vapor Pressure

as compared to the heat of sublimation of neon (at 16°K) of

$$\Delta H_{sNe} = 25 \text{ cal/gm.} \quad (D-2)$$

Therefore, on a weight basis the hydrogen system is definitely superior. On the other hand, the density of solid neon is much greater than solid hydrogen, and as a result a greater volume of solid hydrogen is required for a given heat load than would be required for solid neon.

$$\text{hydrogen} \quad (\Delta H_s) \rho = 10.6 \text{ cal/cm}^3 \quad (D-3)$$

$$\text{neon} \quad (\Delta H_s) \rho = 36.1 \text{ cal/cm}^3. \quad (D-4)$$

A secondary consideration is the vapor pressure level implied by the operating conditions for the two coolants. The vapor pressure of solid hydrogen at the triple point is

$$P_{V_{H_2}} = 54 \text{ torr,} \quad (T = 13.95^\circ K) \quad (D-5)$$

which is the highest possible operating temperature for this particular coolant. The vapor pressure of neon at the same temperature is

$$P_{V_{Ne}} = 0.1 \text{ torr,} \quad (T = 13.95^\circ K) \quad (D-6)$$

and indicates that considerably better vacuum would be required for the use of neon as a coolant at this temperature. The crystal sensor, however, can operate successfully as a mass collector at temperatures as high as 20°K, and since the triple point of neon is above this value ($T_{TP} = 24.57^\circ K$), the neon could be operated at this higher temperature. In this case, the required vapor pressure could be

$$P_{V_{Ne}} = 28 \text{ torr.} \quad (T = 20^\circ K) \quad (D-7)$$

A somewhat better vacuum condition is still required of the neon coolant system as compared to the hydrogen system.

Hydrogen is the most promising substance for this sublimation scheme on the basis of the weight advantage, and because of cost considerations which include the availability at the launch site. In order to avoid a double coolant system, i.e., liquid nitrogen cooling for the collector walls and hydrogen sublimation for crystal cooling, the solid hydrogen volume can be sized to provide sufficient cooling for both functions.

The heat of sublimation plus the crystal heat load implies a hydrogen sublimation rate which in all probability is not matched to the required gaseous heat removal capacity in the 70°K or 100°K temperature range required of the collector walls. Consequently, the greater of the two heat loads will size the mass of solid hydrogen needed for a given flight time, and thus the coolant system will have excess capacity for the lesser heat load. This heat capacity matching poses problems in both situations; i.e., if the collector wall heat load requires the greatest hydrogen gas flow, a heat load beyond that supplied by the crystal must be imposed on the solid hydrogen to maintain the desired sublimation rate. On the other hand, if the crystal heat load is high, the gas flow to the collector may be more than required; this would result in a low collector wall temperature which could begin to act as a condenser, thereby invalidating the crystal sensor measurement. If such is the case, an artificial heat load must be imposed on the subliming gas before it reaches the collector section.

From Section V, the sample gas cooling load plus the heat load due to superinsulation was calculated to be 11.38 milliwatts. Hydrogen gas provides 80 cal/gm cooling capacity between 70°K and 100°K; thus, the required hydrogen sublimation rate for collector cooling is

$$\text{collector} \quad \dot{m} = \frac{11.38 \text{ milliwatt}}{80 \text{ cal/gm}} = 3.39 \times 10^{-5} \text{ gm/sec.} \quad (\text{D-8})$$

The crystal heat load from Section V was 1.037 milliwatts with negligible heat loss due to insulation. The required sublimation rate for the crystal is thus

$$\text{crystal} \quad \dot{m} = \frac{1.037 \text{ milliwatt}}{125 \text{ cal/gm}} = 2.6 \times 10^{-6} \text{ gm/sec.} \quad (\text{D-9})$$

The collector cooling therefore requires the greater hydrogen gas flow; however, there should be no problem in providing the desired sublimation rate by proper design of the superinsulation section surrounding the solid hydrogen (Figure D-2).

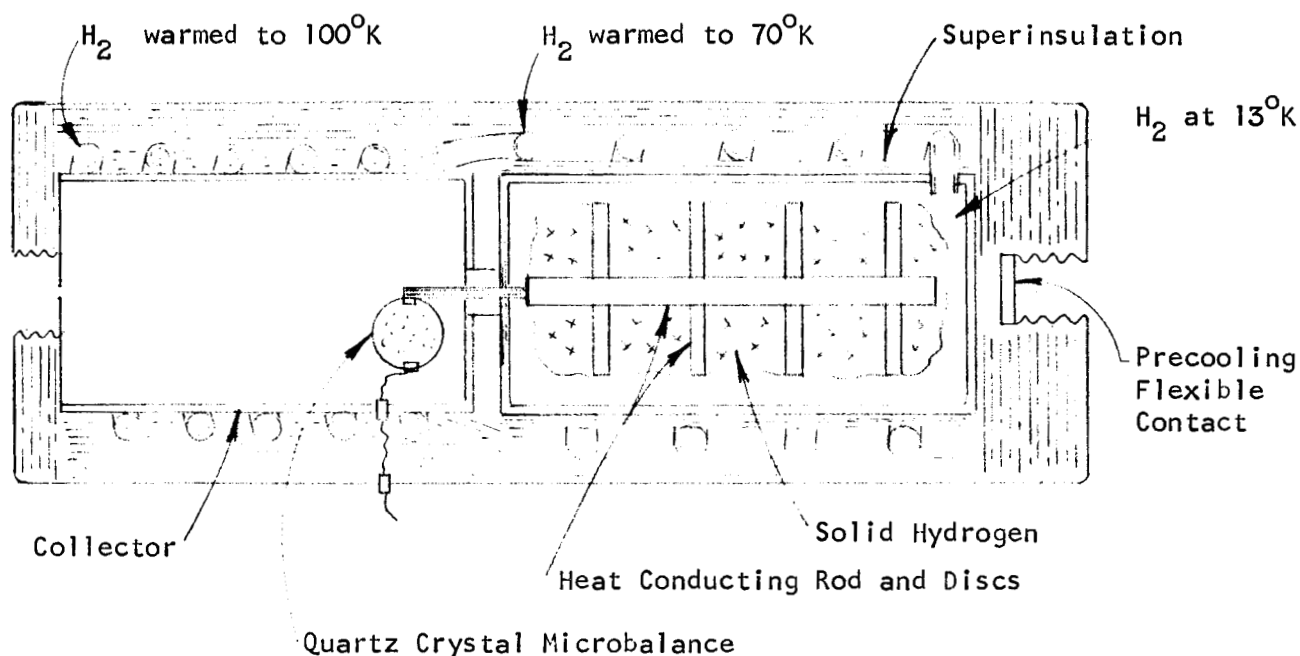


Figure D-2. Hydrogen Sublimation Coolant System

The sublimed gas can be circulated through an intermediate layer of the superinsulation thus providing the proper temperature gradient in the superinsulation for the desired sublimation rate, and at the same time, warming the hydrogen to 70°K before entering the collector coolant section. The required volume of solid hydrogen for a given flight time is

$$V_{\text{solid H}_2} (\text{cm}^3) = \frac{3.39 \times 10^{-5} t}{\rho} = 3.94 \times 10^{-4} t. \quad (\text{D-10})$$

For the hypothetical mission considered in this report $t = 3.57 \times 10^5$ seconds and the required volume is 140.5 cm^3 .

The maintenance of a constant vapor pressure over the solid hydrogen should pose no problems during the vehicle flight. The major heat loads are radiation loads and superinsulation losses and are invariant with time and vehicle altitude; thus, the sublimation rate will remain approximately constant during the flight, and an orifice in the exhaust line can be sized to set the desired vapor pressure for the mass flow rate.

Since the collector is evacuated before launch, the heat loads on the launch pad are essentially the same as the flight conditions. Maintaining the sub-atmospheric vapor pressure that is required if the hydrogen is to remain in a solid phase presents a problem, however, during any unattended hold periods, since the subliming hydrogen cannot be conveniently exhausted by the atmosphere as it can in flight. Neither can the system simply be capped off after evacuation since a 10-liter volume would be required to hold the vapor pressure below 54 torr during a 12-hour hold period.

An alternate approach would be a liquid fill and liquid phase boil-off to the atmosphere during the ground hold period followed by solidification at flight altitude as the liquid hydrogen is exposed to vacuum conditions. Adverse experience with hydrogen vent line plugging by freezing at high altitude would indicate that extreme care would need to be taken in the design and prototype development to avoid losing all the liquid before any solidification in the hydrogen container takes place.

The most reliable hydrogen system would require continuous vacuum pumping during the ground hold period followed by orifice-controlled venting to vacuum while in flight.

REFERENCES

1. Wallace, D. A. and K. W. Rogers, "Design of Molecular Traps for the High-Speed Pumping of Directional Low-Density Nozzle Flow," *Advances in Cryogenic Engineering*, Vol. 9, 1964.
2. Ballance, James O., George C. Marshall Space Flight Center, private communication.
3. Wainwright, J. B. and K. W. Rogers, "Impact Pressure Probe Response Characteristics in High Speed Flows with Transition Knudsen Numbers," University of Southern California Engineering Center, Report 101-101, November 1964.
4. Waters, P. M., and P. O. Raynor, "A Quartz Crystal Microbalance," Westinghouse Research Report 62-115-454-R2, Pittsburg, Pa., Oct. 1962.
5. Stephens, J. B., "Cryogenic Quartz Crystal Microbalance," JPL Space Programs Summary No. 37-30, Vol. IV, p. 79.
6. Stephens, J. B., "Quartz Crystal Microbalance," JPL Space Programs Summary No. 37-34, Vol. IV.
7. Jacobs, R. B., "Liquid Requirements for the Cooldown of Cryogenic Equipment," *Proceedings of the 1962 Cryogenic Engineering Conference*, August 1962.
8. Wang, E. S. J., et al., "The Measurement of the Speed of Cryopumps," *Transactions of the Tenth National Vacuum Symposium of the American Vacuum Society*, October 1963.
9. Buffham, B. A., et al., "A Theoretical Evaluation of the Sticking Coefficient in Cryopumping," *Transactions of the Ninth Vacuum Symposium*, November 1962.
10. Dawson, J. P., "Prediction of Cryopumping Speeds in Space Simulation Chambers," *Transactions of the Ninth Vacuum Symposium*, November 1962.
11. Bachler, W., et al., "Cryogenic Pump Systems Operating Down to 2.5°K," *Transactions of the Ninth Vacuum Symposium*, November 1962.
12. Stickney, W. W. and B. B. Dayton, "The Measurement of the Speed of Cryopumps," *Transactions of the Tenth National Vacuum Symposium of the American Vacuum Society*, October 1963.

REFERENCES (Continued)

13. Roder, H. M., "The Thermal Conductivity of Solid Nitrogen," Cryogenics, Vol. 2., No. 5, September 1962.
14. McCarroll, B. and G. Ehrlich, "Trapping and Energy Transfer in Atomic Collisions with a Crystal Surface," Journal of Chemical Physics, January 1963.
15. Mayer, E., et al., "Condensation of Rarefied Supersonic Flow Incident on a Cold Flat Plate," Fourth International Symposium on Rarefied Gas Dynamics, July 1964.
16. Oman, R. A., et al., "Theoretical Prediction of Momentum and Energy Accommodation for Hypervelocity Gas Particles on an Ideal Crystal Surface," Fourth International Symposium on Rarefied Gas Dynamics, July 1964.
17. Rogers, M., "Analog Computer Studies of Particle Surface Interactions," Fourth International Symposium on Rarefied Gas Dynamics, July 1964.
18. Stuart, R. B., "Sputtering Yields at Medium and Low Energies," Transactions of the Eighth Vacuum Symposium and Second International Congress, October 1961.

AN ORBITING DENSITY MEASURING INSTRUMENT


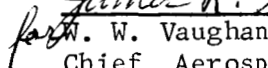
By D. A. Wallace, K. W. Rogers, J. B. Wainwright and R. L. Chuan

The information in this report has been reviewed for security classification. Review of any information concerning Department of Defense or Atomic Energy Commission programs has been made by the MSFC Security Classification Officer. This report, in its entirety, has been determined to be unclassified.

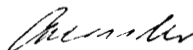
This document has also been reviewed and approved for technical accuracy.



R. E. Smith
Chief, Space Environment Branch

W. W. Vaughan
Chief, Aerospace Environment Division



E. D. Geissler
Director, Aero-Astrodynamics Laboratory